



## A mixture of dicyclohexylamine and oleylamine as a corrosion inhibitor for mild steel in NaCl solution saturated with CO<sub>2</sub> under both continual immersion and top of the line corrosion

IVANA JEVREMOVIĆ<sup>1#</sup>, ALEKSANDRA DEBELJKOVIĆ<sup>1</sup>, MARC SINGER<sup>2</sup>,  
MOHSEN ACHOUR<sup>3</sup>, SRDAN NEŠIĆ<sup>2</sup> and VESNA MIŠKOVIĆ-STANKOVIĆ<sup>1#\*</sup>

<sup>1</sup>University of Belgrade, Faculty of Technology and Metallurgy, Kargujeva 4, 11000 Belgrade, Serbia, <sup>2</sup>Institute for Corrosion and Multiphase Technology, Ohio University, 342 West State St., Athens, OH 45701, USA and <sup>3</sup>ConocoPhillips Company, 226 Geosciences Building, Bartlesville, OK, USA

(Received 22 February, revised 21 May 2012)

**Abstract:** This paper presents a comprehensive method to evaluate a mixture of dicyclohexylamine and oleylamine (DCHA+OA) as a corrosion inhibitor for mild steel in a CO<sub>2</sub> environment in the liquid and vapor phase. The volatile properties of the corrosion inhibitor were investigated in order to determine whether DCHA+OA could be used to control the severity of a top of the line (TLC) corrosion attack. Corrosion measurements were performed using electrochemical impedance spectroscopy, linear polarization resistance, potentiodynamic sweep measurements, as well as electrical resistance and weight loss measurements, in order to determine the inhibitive performances of dicyclohexylamine and oleylamine. In order to define the surface morphological characteristics, the scanning electron microscopy technique was applied. The electrochemical study and the weight loss measurements indicated that DCHA+OA significantly decreased the corrosion rate in the liquid phase when 50 ppm of DCHA+OA was added. Scanning electron microphotographs indicated a protective inhibitor film was formed on the steel surface and revealed that good protection was achieved, together with a decrease in the corrosion rate, as determined by weight loss and electrochemical techniques. It was shown using electrical resistance measurements in the vapor phase, that a concentration of 1000 ppm DCHA+OA significantly decreased the corrosion rate at the top of the line only when it was carried there within its own foam and not due to its volatility.

**Keywords:** carbon steel; corrosion inhibitors; electrochemical measurements; scanning electron microscopy; electrical resistance measurements.

\* Corresponding author. E-mail: vesna@tmf.bg.ac.rs

# Serbian Chemical Society member.

doi: 10.2298/JSC120222058J

## INTRODUCTION

In wet gas transportation, one of the most significant internal corrosion challenges is the so-called Top of the Line Corrosion (TLC). When the fluid stream is cooled, water vapor condenses on the sides and at the top of the line, creating droplets that are very corrosive since they contain dissolved corrosive gases such as CO<sub>2</sub> and H<sub>2</sub>S. It is difficult to mitigate this type of corrosion, as conventional corrosion inhibitors dissolved in the liquid phase cannot be easily transported to the top of the line.<sup>1–5</sup> One possible solution may be the application of volatile corrosion inhibitors (VCI), which have been successfully used in different applications. The advantage of VCI is that the vaporized inhibitor molecules can reach the top of the line and form a relatively stable and protective layer on the metal surface.<sup>6–8</sup>

An aqueous carbon dioxide-saturated system is by far one of the most common corrosive environments encountered in the oil and gas industry.<sup>9–11</sup> The problems arising from CO<sub>2</sub> corrosion have led to the development of various methods of corrosion control and one of the most practical methods for protection is the addition of organic substances as corrosion inhibitors, especially in acidic media.<sup>12–14</sup> Injected inhibitor liquids are carried along the line, thereby producing a protective film all over the internal pipeline surface.<sup>15</sup> Most of the inhibitors are organic heterocyclic compounds with N, S, or O atoms.<sup>16–23</sup> The sites of these elements have higher electron density, so they are considered to be adsorption reaction centers. It was found that most of the organic inhibitors act by adsorption on the metal surface and by blocking the active corrosion sites.<sup>24–26</sup> Inhibitors adsorb on the metal surface by displacing water molecules on the surface and forming a compact film as a physical barrier to reduce the transport of corrosive species to the metal surface.<sup>27</sup> This phenomenon is influenced by the nature and surface charge of the metal, by the type of aggressive electrolyte and by the chemical structure of the inhibitors.<sup>28</sup> As most corrosion inhibitors are required to partition to the water phase, the surface tension between the oil/water interface must be lowered, which is achieved by the addition of a surfactant.<sup>29–31</sup>

In this study, electrochemical impedance spectroscopy (EIS), linear polarization resistance (LPR), potentiodynamic sweep (PDS) measurements, as well as electrical resistance (ER) and weight loss (WL) measurements and scanning electron microscopy (SEM) were conducted in order to investigate the efficiency of a mixture of dicyclohexylamine and oleylamine (DCHA+OA) as a corrosion inhibitor for mild steel in a CO<sub>2</sub> environment in the liquid and vapor phase. Dicyclohexylamine is used for its corrosion inhibition properties, while the oleylamine is used for its surfactant properties. A mixture of DCHA+OA was chosen considering the fact that dicyclohexylamine has a relatively high vapor pressure (1.6 kPa) and good inhibition properties in the liquid phase; hence, it was anticipated that even a small concentration of dicyclohexylamine in the vapor phase



could provide sufficient inhibition at the top. Oleylamine, known as a surfactant, was added in the mixture in order to maximize the contact surface area between dicyclohexylamine and the aqueous medium. In addition, dicyclohexylamine is a water insoluble inhibitor and a surface-active agent, oleylamine, was added to increase surface area and to cause a micro emulsion to form in the water phase. The molecular structures of inhibitor components are shown in Fig. 1.

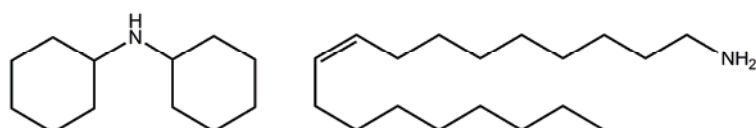
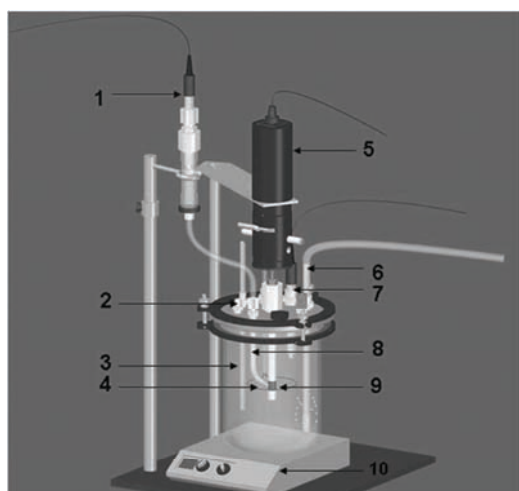


Fig. 1. Molecular structures of dicyclohexylamine and oleylamine.

## EXPERIMENTAL

### *Investigation of the efficiency of the corrosion inhibitor in the liquid phase*

The carbon steel API X65 was used in all experiments. The test specimens of surface area 5.4 cm<sup>2</sup>, were sequentially polished using 240, 320, 400 and 600 grit silicon carbide paper, rinsed with 2-propanol in an ultrasonic cleaner for 1 to 2 minutes and then air-dried. The mixture of corrosion inhibitor dicyclohexylamine and oleylamine (1:1 vol. %) in a concentration of 50 ppm was added to a 3 wt. % NaCl solution. The cell temperature was monitored by a thermocouple. When the required temperature was achieved, the pH of the test solution was adjusted by addition of a deoxygenated sodium bicarbonate solution. The linear polarization resistance, electrochemical impedance spectroscopy, potentiodynamic sweep and weight loss measurements were performed in a glass cell, shown in Fig. 2. The test matrix for this experimental series is shown in Table I.



- |                        |                               |
|------------------------|-------------------------------|
| 1. Reference electrode | 2. Gas outlet                 |
| 3. Temperature probe   | 4. Platinum counter electrode |
| 5. Rotator             | 6. Gas inlet                  |
| 7. pH - electrode      | 8. Luggin capillary           |
| 9. Working electrode   | 10. Hot plate                 |

Fig. 2. Scheme of the glass cell for the CO<sub>2</sub> corrosion test of mild steel.<sup>9</sup>

TABLE I. Test matrix for the CO<sub>2</sub> experiments in the liquid phase

Parameter	Value
Total pressure, kPa	100
CO <sub>2</sub> partial pressure, kPa	96 and 69
Liquid temperature, °C	20 and 70
NaCl solution, wt. %	3
Concentration of DCHA+OA, ppm	50
pH	5
Measurements	OCP, EIS, LPR, PDS

*Electrochemical measurements.* All the electrochemical measurements were performed using a Gamry, Reference 600 potentiostat/galvanostat/ZRA. An Ag/AgCl (4M KCl) reference electrode was externally connected *via* a Luggin capillary. The counter electrode was a concentric platinum wire. The open circuit potential was monitored for 30 min, in which time a stable potential was reached, before all the electrochemical measurements were realized. The electrochemical measurements were typically conducted in the same order: linear polarization resistance, electrochemical impedance spectroscopy and potentiodynamic sweep. The linear polarization resistance (LPR) measurements were performed from a cathodic potential of -5 mV to an anodic potential of +5 mV, with respect to the corrosion potential, at a scan rate of 0.125 mV s<sup>-1</sup>. The electrochemical impedance spectroscopy (EIS) measurements were performed over a frequency range of 10 kHz to 10 mHz using a 10 mV amplitude of sinusoidal voltage. The potentiodynamic sweep (PDS) measurements were realized from a cathodic potential of -0.25 V to an anodic potential of 0.25 V, with respect to the corrosion potential, at a scan rate of 0.2 mV s<sup>-1</sup>.

*Weight loss measurements.* Typically after 24 h, pre-weighed samples were taken out of the 3 wt. % NaCl purged with CO<sub>2</sub> gas without and with DCHA+OA at 20 °C, and at 70 °C, rinsed with 2-propanol and wiped with a cloth to remove any salt residue and carbide scales, then air dried and weighed on an analytic balance (accuracy ±0.1 mg).

*Surface morphology.* A scanning electron microscope (SEM) JEOL JSM-6390 was used to analyze the morphology of the mild steel surface. Images of the specimens were recorded after 24 h exposure time in 3 wt. % NaCl purged with CO<sub>2</sub> gas at 20 °C, and at 70 °C without and with DCHA+OA.

*Electrical resistance measurements.* All measurements were realized using a Microcor Online Corrosion Monitoring System, Rohrback Cosasco Systems. API X65 steel specimens were pretreated with 78 wt. % H<sub>2</sub>SO<sub>4</sub> for 30 s, rinsed with distilled water for 10 s and then polished with emery paper grit 600 and rinsed with distilled water. The solutions were deaerated by purging carbon dioxide gas for an hour before the start of the experiment, and then the bubbler was placed in the vapor phase. CO<sub>2</sub> injection was maintained during the entire test. When the desired conditions were achieved, the ER probe was put into the glass cell and corrosion rate was monitored. The test matrix for this experimental series is shown in Table II.

#### *Investigation of efficiency of the corrosion inhibitor in the vapor phase*

The experiments were performed in a glass cell containing 3 wt. % aqueous NaCl solutions with 1000 ppm of acetic acid added. The test solution was deoxygenated by bubbling CO<sub>2</sub> for an hour and then the CO<sub>2</sub> gas inlet was placed in the vapor phase. At the same time, the temperature was increased to 70 °C. Once the experimental conditions were attained, an



ER probe was installed flush mounted at the bottom of a stainless steel lid. When the bare steel corrosion rate was obtained, 1000 ppm of corrosion inhibitor DCHA+OA was injected into the solution.

TABLE II. Test matrix for the ER measurements

Parameter	Value
Total pressure, kPa	100
CO <sub>2</sub> partial pressure, kPa	69
Liquid temperature, °C	70
NaCl solution, wt. %	3
Concentration of DCHA+OA, ppm	1000
Concentration of acetic acid, ppm	1000
pH	4
Measurement	ER

## RESULTS AND DISCUSSION

### *Efficiency of the corrosion inhibitor in the liquid phase*

The objective of this part of the experiments was to determine the basic properties of the investigated corrosion inhibitor dicyclohexylamine and oleylamine (DCHA+OA) in the liquid phase.

*Electrochemical measurements.* The impedance data were analyzed using the electric equivalent circuit presented in Fig. 3, where  $R_Q$  is the solution resistance,  $C_{dl}$  is the double layer capacitance and  $R_{ct}$  is the charge-transfer resistance.<sup>32–34</sup>

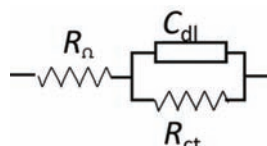


Fig. 3. Electrical equivalent circuit.

The Nyquist plots of the mild steel in 3 wt. % NaCl saturated with CO<sub>2</sub>, pH 5, without and with 50 ppm DCHA+OA, at 20 °C are shown in Fig. 4.

From the Nyquist plots, it could be seen that the impedance response significantly changed on addition of DCHA+OA. The inhibition efficiency ( $IE / \%$ ) after different exposure times was calculated from the impedance data using the following equation:

$$IE / \% = \frac{R_{ct} - R_{0ct}}{R_{ct}} \cdot 100 \quad (1)$$

where  $R_{0ct}$  and  $R_{ct}$  are the charge-transfer resistance values without and with inhibitor, respectively.<sup>35</sup> The values of charge-transfer resistance and inhibition efficiency obtained from the EIS measurements for mild steel in 3 wt. % NaCl at 20 °C and at 70 °C are given in Table III, from which it can be observed that the

inhibition efficiency increased upon addition of 50 ppm of DCHA+OA during the exposure time and reached a maximum inhibition efficiency of 98 % after 49 h of exposure at 20 °C.

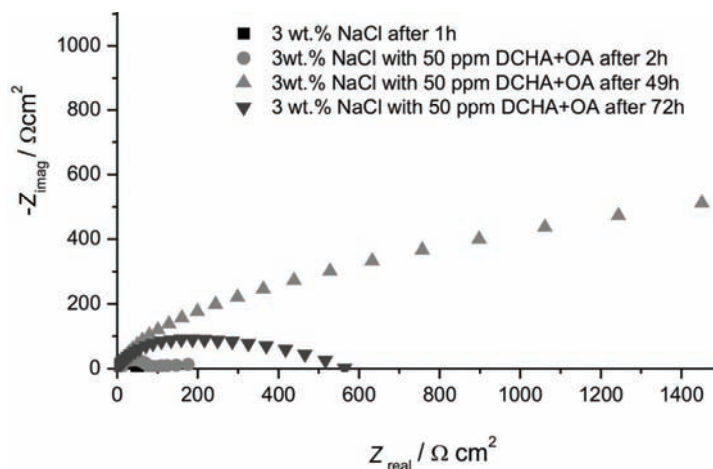


Fig. 4. Nyquist plots for mild steel in 3 wt. % NaCl solution at 20 °C, pH 5, without and with 50 ppm DCHA+OA.

TABLE III. The values of the charge-transfer resistance and inhibition efficiencies obtained from EIS measurements for mild steel in 3 wt. % NaCl solution without and with inhibitor (DCHA+OA), at 20 and 70 °C

<i>c</i> (DCHA+OA) / ppm	<i>t</i> / h	<i>t</i> / °C	<i>R</i> <sub>ct</sub> / Ω cm <sup>2</sup>	<i>IE</i> / %
0	1	20	50	–
50	2	20	90	44
50	49	20	2400	98
50	72	20	600	92
0	1	70	12	–
50	2	70	50	76
50	22	70	500	98
50	32	70	150	92

It can also be seen from Table III that the values of charge-transfer resistance at 20 °C in 3 wt. % NaCl with inhibitor increased with exposure time (up to 49 h), indicating the presence of an inhibitor layer adsorbed at the metal surface that acts as a barrier layer. After prolonged time (72 h), the charge-transfer resistance decreased, which could be explained by desorption of the inhibitor film from the metal surface and lower inhibition performances. A similar behavior was observed at 70 °C, but after shorter exposure times (22 and 32 h, respectively). It appears that inhibitor molecules probably start to desorb during time due to interactions between the inhibitor molecules already adsorbed at the metal surface and those present in solution. With increasing amount of adsorbed inhibitor, the inter-

actions become stronger, leading to secondary desorption after prolonged exposure. As could be expected, the values of the charge-transfer resistance at 70 °C were lower compared to the values at 20 °C due to the faster corrosion process and smaller amount of adsorbed inhibitor. It is well known that the amount of adsorbed inhibitor decreases with increasing temperature.

Similar behavior can be observed from the potentiodynamic sweep curves shown in Fig. 5. The addition of DCHA+OA shifted the corrosion potential to slightly more positive values and decreased the corrosion rate of mild steel. In the absence of inhibitor, the corrosion current density was calculated to be  $8 \times 10^{-5} \text{ A cm}^{-2}$ , which is about 10 times greater than the corrosion current density with inhibitor ( $1.7 \times 10^{-6} \text{ A cm}^{-2}$ ). According to Fig. 5, it appears that DCHA+OA is a mixed-type inhibitor, since it reduces both the cathodic and anodic current densities. The decrease in the corrosion current density and increase in the corrosion potential confirm the inhibition properties of DCHA+OA. However, the rate of anodic dissolution of steel increased in the presence of inhibitor at more positive potentials than -300 mV (Ag/AgCl), which was previously reported as the desorption potential.<sup>18,35</sup>

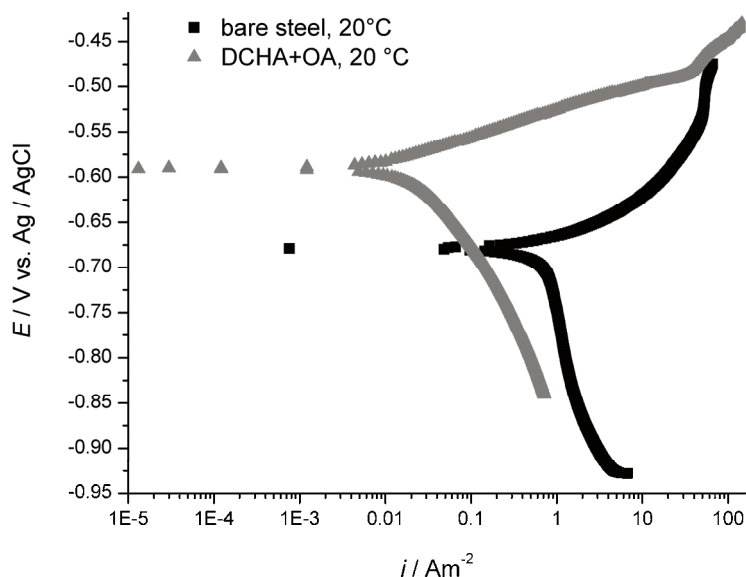


Fig. 5. Polarization curves of mild steel in 3 wt. % NaCl solution at 20 °C, pH 5, without and with 50 ppm DCHA+OA.

The value of  $R_p$  was determined using linear polarization resistance (LPR), while the corrosion rate was calculated using the following equations:

$$i_{\text{corr}} = \frac{1}{A R_p} \frac{b_a b_c}{2.303(b_a + b_c)} \quad (2)$$

$$CR = \frac{M_w}{\rho n F} i_{\text{corr}} \quad (3)$$

where,  $b_a$  and  $b_c$  are the anodic and cathodic Tafel slopes, respectively,  $M_w$  is the molecular weight of iron,  $A$  is the surface area of the sample, which is  $5.4 \text{ cm}^2$ ,  $\rho$  is the density of iron,  $n$  is the number of electrons exchanged in the electrochemical reaction and  $F$  is the Faraday constant. It was found that corrosion rate of mild steel in 3 wt. % NaCl, pH 5, at 20°C decreased to below 0.1 mm yr<sup>-1</sup> when 50 ppm of DCHA+OA was added compared to the corrosion rate of 0.6 mm yr<sup>-1</sup> for bare steel (Fig. 6). The corrosion rate at 70 °C also decreased from 2.2 mm yr<sup>-1</sup> for bare steel to 0.1 mm yr<sup>-1</sup> on addition of 50 ppm of DCHA+OA (Fig. 7). As can be seen in Figs. 6 and 7, the  $E_{\text{corr}}$  value shifted from approximately -0.7 V for the uninhibited system to -0.6 V in the presence of DCHA+OA. Namely,  $E_{\text{corr}}$  shifted to slightly more positive values from that of the uninhibited electrode when corrosion inhibitor was added. In general, DCHA+OA is considered as a mixed type of corrosion inhibitor because it affects both the metal ionization and the hydrogen evolution reaction, but the anodic action is more pronounced.

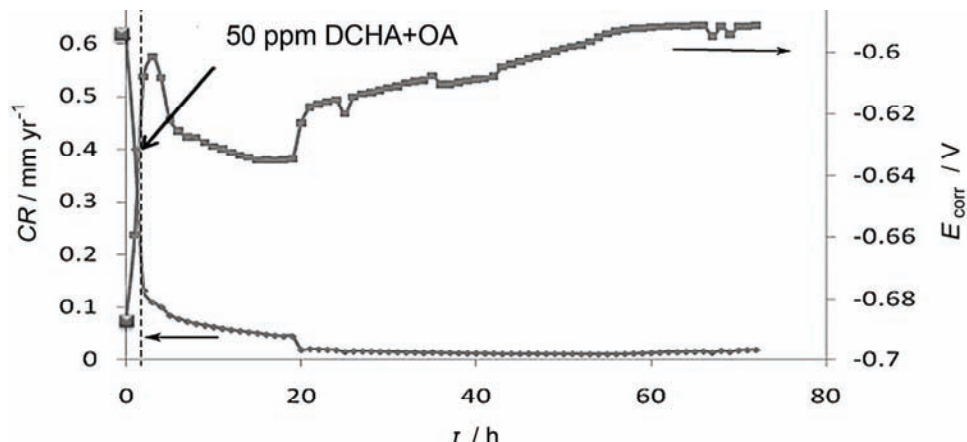


Fig. 6. Corrosion rate and corrosion potential of mild steel in 3 wt. % NaCl solution at 20 °C, pH 5, without and with 50 ppm DCHA+OA, measured by LPR during 72 h.

*Weight loss measurements.* The effect of addition of the DCHA+OA inhibitor on the corrosion of mild steel in 3 wt. % NaCl solution was also studied by weight loss measurements at 20 and 70 °C after a 24-h immersion period. The weight loss method was used in order to estimate average corrosion rates.<sup>36</sup> The weight loss (WL) was calculated from the equation:

$$WL = W_1 - W_2 \quad (4)$$

where  $W_1$  and  $W_2$  are the average weight of the specimens before and after exposure, respectively. The corrosion rate,  $CR$ , was calculated using the equation:

$$CR = \frac{WL}{S\rho t} \quad (5)$$

where,  $S$  is the surface area of specimens,  $\rho$  is the density of iron and  $t$  is the exposure time.<sup>18</sup> It can be seen from Table IV that the corrosion rate significantly decreased on addition of the DCHA+OA corrosion inhibitor at both temperatures. The results obtained from the weight loss measurements are in accordance with the results obtained from the EIS and PDS measurements.

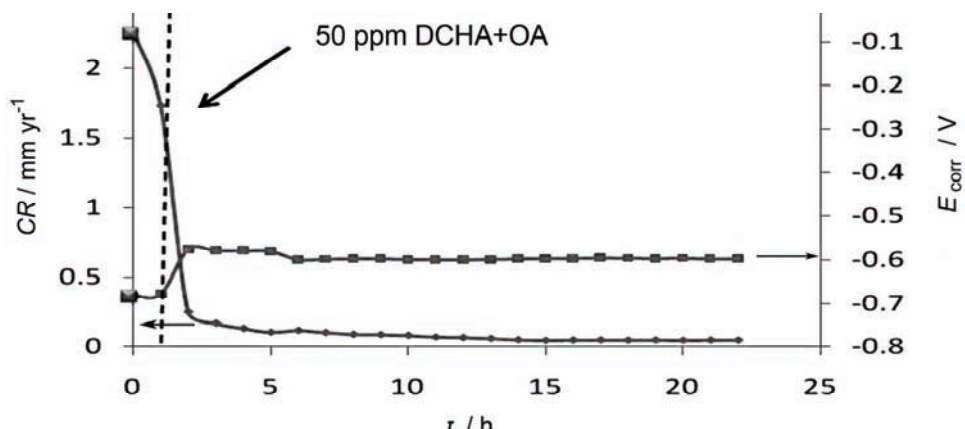


Fig. 7. Corrosion rate and corrosion potential of mild steel in 3 wt. % NaCl solution at 70 °C, pH 5, without and with 50 ppm DCHA+OA, measured by LPR during 24 h.

It can be considered that the inhibition performances of the corrosion inhibitor dicyclohexylamine and oleylamine and the reduced corrosion rate are the consequence of strong interactions established between the N atoms with unshared electron pair from the dicyclohexylamine (DCHA) and oleylamine (OA) molecules and the negatively charged metal surface. Moreover, the long alkyl chains from oleylamine can orientate the inhibitor on the metal surface. In addition, van der Waals interactions are established between the alkyl chains, so they form a firmly adsorbed hydrophobic layer that protects the steel surface against corrosion attack.

*Surface morphology.* The SEM microphotographs of mild steel surface after 24 h of exposure to 3 wt. % NaCl solution without and with DCHA+OA added at 20 °C and at 70 °C are shown in Fig. 8. In the absence of inhibitor (Figs. 8a and b), the mild steel surface was strongly damaged due to metal dissolution in the corrosive solution. The surface after exposure at 20 °C was very rough and uneven

while the specimen that was exposed at 70 °C (Fig. 8b) had deep and large holes at the surface. However, the appearance of steel surface was significantly different after the addition of DCHA+OA to the corrosive solution. As can be seen from Figs. 8c and 8d, the dissolution rate of mild steel was reduced and a uniform, smooth surface appeared due to formation of a protective inhibitor film on the metal surface. The SEM results are in accordance with the results of the weight loss and electrochemical measurements.

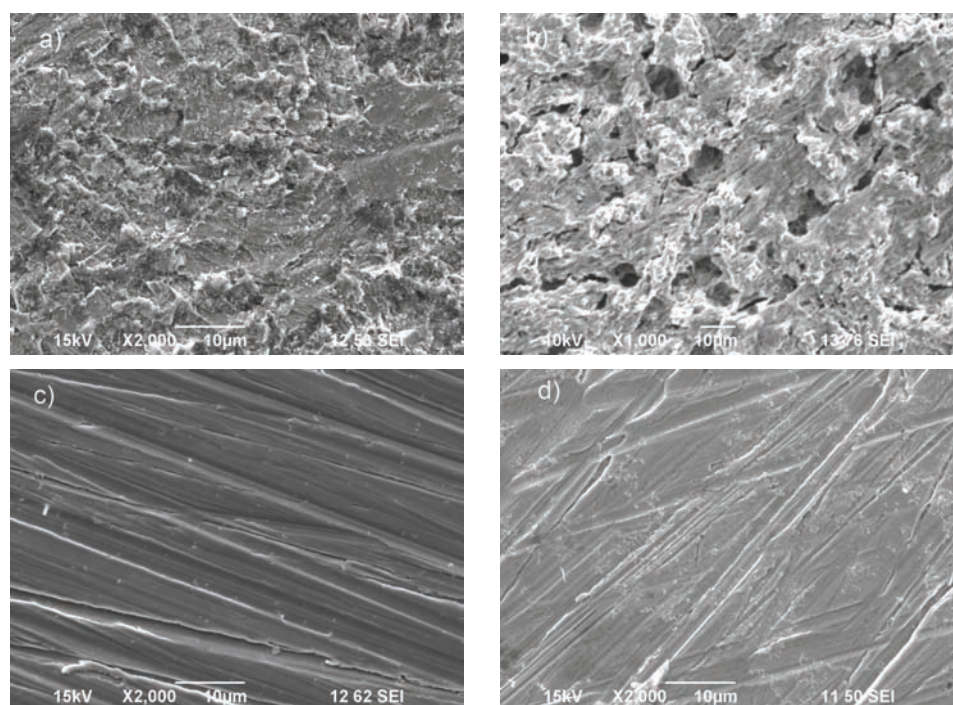


Fig. 8. SEM Microphotographs of mild steel after exposure to 3 wt. % NaCl solution at: a) 20 and b) 70 °C; c) with 50 ppm DCHA+OA at 20 °C and d) with 50 ppm DCHA+OA at 70 °C.

*Electrical resistance measurements.* The time dependences of the decrease metal thickness and corrosion rate when 1000 ppm DCHA+OA was added in 3 wt. % NaCl solution are shown in Fig. 9, indicating that the corrosion rate after 20 h was around  $0.1 \text{ mm yr}^{-1}$ . After the baseline conditions were established, the corrosion rate of bare steel in solution was around  $4.5 \text{ mm yr}^{-1}$ . Consequently, it can be considered that a concentration of 1000 ppm DCHA+OA significantly decreased the corrosion rate in the liquid phase. Similar results were obtained using LPR (Fig. 7) and weight loss measurements (Table IV).

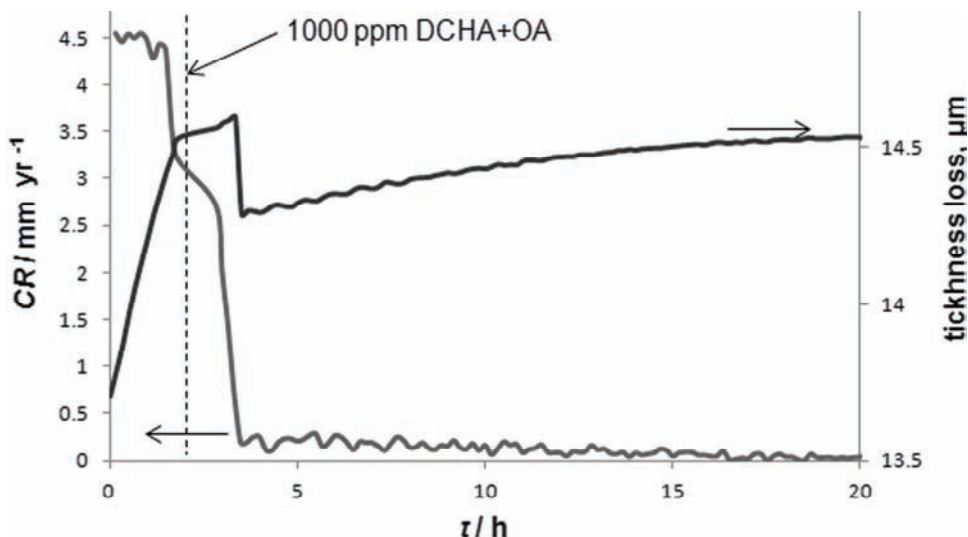


Fig. 9. The time dependence of the decrease in metal thickness and corrosion rate for mild steel in the liquid phase when 1000 ppm DCHA+OA was added to 3 wt. % NaCl solution at 70 °C, pH 4, with 1000 ppm of acetic acid.

TABLE IV. Weight loss measurements after 24 h for mild steel in 3 wt. % NaCl solution without and with inhibitor (DCHA+OA), at 20 and 70 °C

c (DCHA+OA) / ppm	t / °C	WL / mg	CR / mm yr <sup>-1</sup>
0	20	0.017	0.96
50	20	0.0002	0.012
0	70	0.074	4.3
50	70	0.0016	0.095

#### *Efficiency of the corrosion inhibitor in the vapor phase*

The aim of this part of the study was to investigate the volatile properties of the corrosion inhibitor DCHA+OA using electrical resistance (ER) measurements. The time dependences of the decrease in the metal thickness and the corrosion rate in vapor phase when 1000 ppm DCHA+OA was added to a 3 wt. % NaCl solution are shown in Fig. 10. The rate of decrease of the metal thickness was constant when 1000 ppm of corrosion inhibitor DCHA+OA was injected (Fig. 10), indicating that the inhibitor DCHA+OA has poor volatile properties and did not protect the carbon steel at the top of the line.

The corrosion rate increased during the first 2 h and reached approximately 0.5 mm yr<sup>-1</sup> (Fig. 10). After the corrosion rate of bare steel was established, 1000 ppm of corrosion inhibitor DCHA+OA was injected directly into the solution. It can be seen that the added inhibitor had no effect on the corrosion rate in the vapor phase.

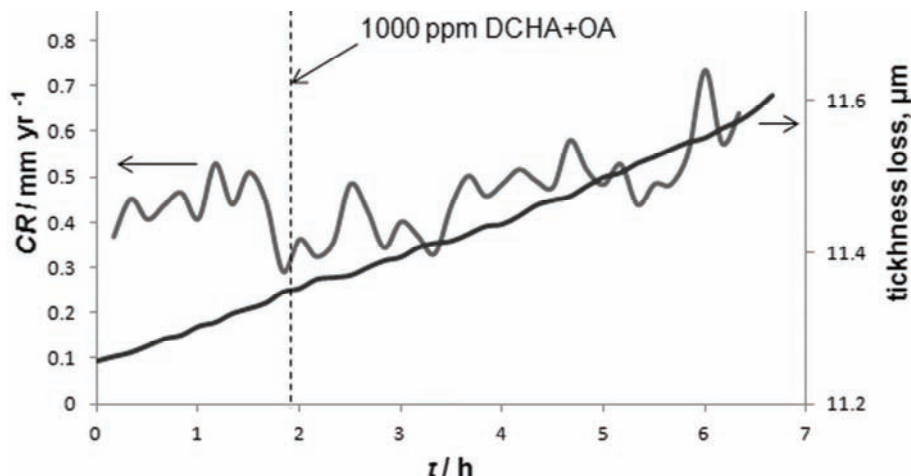


Fig. 10. The time dependence of the decrease in metal thickness and corrosion rate for mild steel in the vapor phase when 1000 ppm DCHA+OA was added to 3 wt. % NaCl solutions at 70 °C, pH 4, with 1000 ppm of acetic acid.

In an additional experiment foam was created inside the glass cell by placing the bubbler in the liquid phase instead of in the vapor phase after addition of the corrosion inhibitor DCHA+OA to the solution. The time dependences of the decrease in the metal thickness and the corrosion rate in vapor phase when foam was created after the addition of 1000 ppm DCHA+OA to the 3 wt. % NaCl solution are shown in Fig. 11.

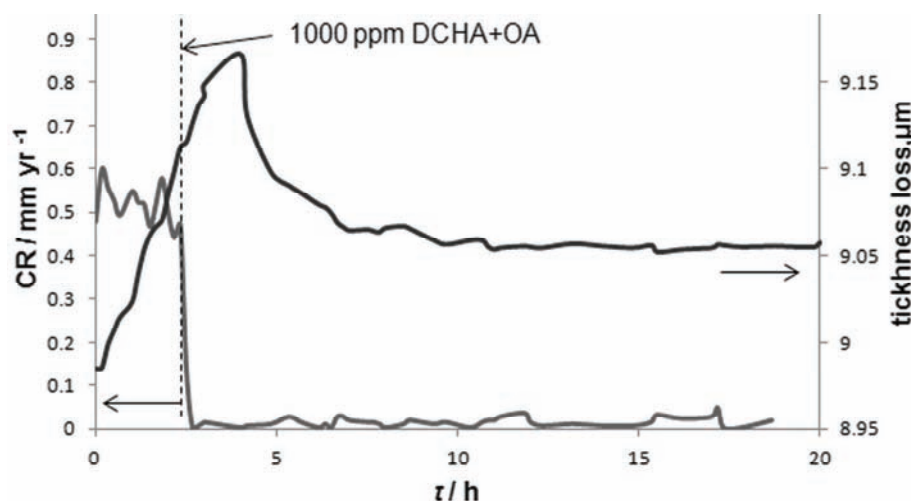


Fig. 11. The time dependence of the decrease in metal thickness and corrosion rate for mild steel in the vapor phase with foam created when 1000 ppm DCHA+OA was added to 3 wt. % NaCl solution at 70 °C, pH 4 with 1000 ppm of acetic acid.

The corrosion rate in the vapor phase increased during the first 2.5 h and reached approximately  $0.5 \text{ mm yr}^{-1}$  and then decreased to below  $0.1 \text{ mm yr}^{-1}$  after the foam contacted the ER probe (Fig. 11). Consequently, it could be concluded that a concentration of 1000 ppm DCHA+OA significantly decreased the corrosion rate at the top only when it was carried to the top within its own foam and not due to its volatility.

#### CONCLUSIONS

The electrochemical study of the efficiency of the corrosion inhibitor dicyclohexylamine and oleylamine (DCHA+OA) in liquid phase showed that the corrosion rate of mild steel in 3 wt. % NaCl solution at pH 5 and at  $20^\circ\text{C}$  decreased to below  $0.1 \text{ mm yr}^{-1}$  when 50 ppm of DCHA+OA was added, compared to bare steel corrosion rate of  $0.6 \text{ mm yr}^{-1}$ . The corrosion rate also decreased from  $2.2 \text{ mm yr}^{-1}$  for bare steel to  $0.1 \text{ mm yr}^{-1}$  by adding 50 ppm of DCHA+OA at  $70^\circ\text{C}$ . The protective action of the added inhibitor can be explained by the strong interactions established between the unshared electron pair of the N atoms of the dicyclohexylamine (DCHA) and oleylamine (OA) molecules and the negatively charged metal surface. Scanning electron microphotographs of mild steel surface also revealed that DCHA+OA inhibits the corrosion process and a uniform, smooth surface appeared due to formation of a protective inhibitor film on the metal surface. Electrical resistance measurements in the liquid phase showed that the corrosion rate at  $70^\circ\text{C}$  after 20 h was below  $0.1 \text{ mm yr}^{-1}$  when 1000 ppm of DCHA+OA was added. From electric resistance measurements in the vapor phase, it could be concluded that the inhibitor DCHA+OA has poor volatile properties and does not protect the carbon steel at the top of the line. On the other hand, it was shown that a concentration of 1000 ppm DCHA+OA significantly decreased the corrosion rate at the top when it was carried to the top within its own foam.

*Acknowledgements.* The authors would like to express their gratitude to ConocoPhillips, USA, and the Ministry of Education, Science and Technological Development of the Republic of Serbia (Grant No. III 45019) for financial support.

#### ИЗВОД

СМЕСА ДИЦИКЛОХЕКСИЛАМИНА И ОЛЕИЛАМИНА КАО ИНХИБИТОР КОРОЗИЈЕ НИСКОУГЉЕНИЧНОГ ЧЕЛИКА У РАСТВОРУ  $\text{NaCl}$  ЗАСИЋЕНОМ СА  $\text{CO}_2$

ИВАНА ЈЕВРЕМОВИЋ<sup>1</sup>, АЛЕКСАНДРА ДЕБЕЉКОВИЋ<sup>1</sup>, MARC SINGER<sup>2</sup>, MOHSEN ACHOUR<sup>3</sup>,  
СРЂАН НЕШИЋ<sup>2</sup> и ВЕСНА МИШКОВИЋ-СТАНКОВИЋ<sup>1</sup>

<sup>1</sup>Технолошко-мештапурички факултет, Универзитет у Београду, Карнеијева 4, Београд, <sup>2</sup>Institute for Corrosion and Multiphase Technology, Ohio University, 342 West State St., Athens, OH 45701, USA и

<sup>3</sup>ConocoPhillips Company, 226 Geosciences Building, Bartlesville, OK, USA

У овом раду испитивана је заштита нискоугљеничног челика од корозије под дејством  $\text{CO}_2$  применом смесе дициклохексиламина и олеиламина (DCHA+OA) као инхи-



битора у течној и гасовитој фази. Испарљивост смесе DCHA+OA је испитивана у циљу потенцијалне примене DCHA+OA као лако испарљивог инхибитора за смањење брзине корозије у условима кондензације. При испитивању инхибиторских својстава смесе дигиклохекциламина и олеиламина примењене су следеће технике карактеризације: спектроскопија електрохемијске импедансије, метода линеарне поларизационе отпорности, метода поларизације линеарно променљивим потенцијалом, мерење електричне отпорности, гравиметријска метода одређивања губитка масе, као и скенирајућа електронска микроскопија. Резултати електрохемијских мерења и гравиметријске методе одређивања губитка масе показују да додата смеса DCHA+OA у концентрацији од 50 ppm значајно смањује брзину корозије у течној фази у односу на систем без инхибитора. Микрофотографије површине челика потврђују да се у присуству смесе DCHA+OA смањује степен корозије као последица формирања заштитног филма инхибитора на површини нискоугљеничног челика. Применом технике мерења електричне отпорности у гасовитој фази показано је да додатак смесе инхибитора DCHA+OA у концентрацији од 1000 ppm доводи до значајног смањења брзине корозије у условима кондензације, само у случају када се транспорт инхибитора до површине челика остварује у облику пене, а не због испарљивости самог инхибитора.

(Примљено 22. фебруара, ревидирано 21. маја 2012)

#### REFERENCES

1. F. Vitse, S. Nesic, Y. Gunaltun, D. Larrey de Torreben, P. Duchet-Suchaux , *Corrosion* **59** (2003) 1075
2. Z. Zhang, D. Hinkson, M. Singer, H. Wang, S. Nesic, *Corrosion* **63** (2007) 1051
3. M. Singer, A. Camacho, B. Brown, S. Nesic, *Corrosion* **67** (2011) B1
4. D. Hinkson, Z. Zhang, M. Singer, S. Nesic, *Corrosion* **66** (2010) A1
5. I. Jevremović, M. Singer, M. Achour, D. Blumer, T. Baugh, V. Mišković-Stanković, S. Nešić, *Corrosion* (2012), <http://dx.doi.org/10.5006/0617>
6. E. Cano, D. M. Bastidas, J. Simancas, J. M. Bastidas, *Corrosion* **61** (2005) 473
7. D. M. Bastidas, E. Cano, E. M. Mora, *Anti-Corros. Meth. M.* **52** (2005) 71
8. R. L. Martin, *Mater. Perform.* **48** (2009) 48
9. F. Haitao, *Low temperature and high salt concentration effect on general CO<sub>2</sub> corrosion for carbon steel*, MS thesis, The Russ College of Engineering and Technology of Ohio University (2006).
10. X. Liu, Y. G. Zheng, *Corros. Eng. Sci. Techn.* **43** (2008) 87
11. L. Zhaoling, F. Chaoyang, G. Xingpeng, *Anti-Corros. Meth. M.* **54** (2007) 301
12. F. Bentiss, M. Lagrenée, M. Traisnel, J. C. Hornez, *Corros. Sci.* **41** (1999) 789
13. G. Achary, H. P. Sachin, Y. A. Naik, T. V. Venkatesha, *Mater. Chem. Phys.* **107** (2008) 44
14. S. D. Shetty, P. Shetty, H. V. S. Nayak, *J. Serb. Chem. Soc.* **71** (2006) 1073
15. S. Nesic, *Corros. Sci.* **49** (2007) 4308
16. S. A. Ali, M. T. Saeed, S. U. Rahman, *Corros. Sci.* **45** (2003) 253
17. A. Döner, G. Kardas, *Corros. Sci.* **53** (2011) 4223
18. A. Döner, R. Solmaz, M. Özcan, G. Kardas, *Corros. Sci.* **53** (2011) 2902.
19. V. R. Saliyan, A. V. Adhikari, *Corros. Sci.* **50** (2008) 55
20. F. Bentiss, M. Traisnel, H. Vezin, H. F. Hildebrand, M. Lagrenée, *Corros. Sci.* **46** (2004) 2781



21. M. El. Azhar, B. Mernari, M. Traisnel, F. Bentiss, M. Lagrenée, *Corros. Sci.* **43** (2001) 2229
22. M. Finšgar, I. Milošev, *Mater. Corros.* **62** (2011) 956
23. M. Finšgar, J. Kovač, I. Milošev, *J. Electrochem. Soc.* **157** (2010) C52
24. B. Wang, M. Du, J. Zhang, C. J. Gao, *Corros. Sci.* **53** (2011) 353
25. D. M. Dražić, Lj. Vračar, V. J. Dražić, *Electrochim. Acta* **39** (1994) 1165
26. Lj. M. Vračar, D. M. Dražić, *Corros. Sci.* **44** (2002) 1669
27. M. Lebrini, M. Lagrene, H. Vezin, L. Gengembre, F. Bentiss, *Corros. Sci.* **47** (2005) 485
28. R. A. Prabhu, T. V. Venkatesha, A. V. Shanbhag, G. M. Kulkarni, R. G. Kalkhambkar, *Corros. Sci.* **50** (2008) 3356
29. W. Wang, M. L. Free, *Corros. Sci.* **46** (2004) 2601
30. M. L. Free, *Corros. Sci.* **44** (2002) 2865
31. M. L. Free, *Corros. Sci.* **46** (2004) 3101
32. W. Guo, S. Chen, H. Ma, *J. Serb. Chem. Soc.* **71** (2006) 167
33. J. B. Bajat, V. B. Mišković-Stanković, *Prog. Org. Coat.* **49** (2004) 183
34. J. B. Bajat, V. B. Mišković-Stanković, Z. Kačarević-Popović, *Prog. Org. Coat.* **47** (2003) 49
35. A. Chetouani, A. Aouniti, B. Hammouti, N. Benchat, T. Benhadda, S. Kertit, *Corros. Sci.* **45** (2003) 1675
36. S. Muralidharan, M. A. Quraishi, S. V. K. Iyer, *Corros. Sci.* **37** (1995) 1739.

